**Article:**

Sun, J., Li, P. and Susmel, L. orcid.org/0000-0001-7753-9176 (2023) The theory of critical distances for random vibration fatigue life analysis of notched specimens. Fatigue and Fracture of Engineering Materials and Structures, 46 (10). pp. 3610-3621. ISSN 8756-758X

https://doi.org/10.1111/ffe.14088

# The Theory of Critical Distances for random vibration fatigue life analysis of notched specimens

Jiachen Sun [1] Piao Li [2*] Luca Susmel[2]

(1 *College of Aeronautics and Astronautics, Nanjing 210016, China*)

(2 *Department of Civil and Structural Engineering, The University of Sheffield, Sheffield S1 3JD, UK*)

**Abstract**

In this paper the Theory of Critical Distances (TCD) is reformulated to be employed to estimate random vibration fatigue lifetime of notched components. Using the Point Method argument, the response stress at the critical distance from the notch root is taken as the damage parameter and then used to perform the vibration fatigue life analysis in the presence of geometrical features. First, the finite element simulation is conducted to obtain the response Mises stress power spectrum at the critical distance under the load excitation being investigated. Subsequently, the probability density distribution of the stress amplitude at this position is calculated. Finally, fatigue lifetime is predicted via the parent material *S-N* curve. In order to check the accuracy of the proposed reformulation of the TCD, a series of random vibration fatigue results were generated by testing notched aluminum alloy specimens under load spectra covering the 1st, 2nd and 3rd order natural frequencies. The results from the vibration fatigue tests being performed are seen to be in sound agreement with the predicted lifetimes. This strongly support the idea that the TCD is successful also in predicting random vibration fatigue lifetime of notched components.

**KEYWORDS**

Critical Distance, Random vibration fatigue, Aluminum alloy, Notch, Mises stress spectrum

## 1. INTRODUCTION

Vibration fatigue is a common failure mode of engineering structures. Stress

* Corresponding author. E-mail address: lipiao@nuaa.edu.cn

concentrations introduced by holes or connections are inevitable in engineering. Therefore, it is of great significance to study the impact of notched stress concentration under vibration fatigue conditions.

Generally, there are two ways to estimate the structural vibration fatigue life: time domain method and frequency domain method. The time domain method refers to obtaining the time history of the response stress or strain at the dangerous point of the structure, and then the cycle counting method is used for cycle counting processing. Finally, the fatigue life is estimated according to the *S-N* curve and the fatigue cumulative damage theory. The frequency domain method expresses the amplitude by using response stress/strain spectral parameters, and then combines the *S-N* curve of materials and the fatigue cumulative damage theory to estimate the life.

For conventional fatigue, the commonly used fatigue life analysis methods for notched specimens include, amongst other, the nominal stress method [1], the stress field intensity method [2-4], and the Theory of Critical Distances (TCD) [5,6].

The differences between vibration fatigue and conventional fatigue lie in the stress/strain analysis and life estimation methods. Vibration fatigue belongs to dynamic response analysis, and the response stress of the structure depends on the amplitude of external loads and the dynamic characteristics of the structures. However, conventional fatigue analysis rarely involves the acceleration of loads. In terms of life estimation methods, vibration fatigue requires the statistical information of the stress/strain to estimate fatigue life, which is not considered in conventional fatigue.

Despite all these, the material fatigue failure mechanisms of both are consistent, and the initiation and propagation process of fatigue cracks are also identical. Therefore, conventional fatigue life analysis methods can be used as reference for vibration fatigue life analysis. The keys to vibration fatigue analysis are response stress spectrum and stress possibility density function at dangerous point or nominal stress point. Using the nominal stress method or the local stress strain method, the vibration fatigue life analysis of smooth or notched parts can be achieved by introducing a mean square stress concentration factor, which is well described in [1].

To solve the problem of vibration fatigue, scholars have carried out relevant research on the basis of the above methods.Wirsching PH et al [7] used rain-flow method to conduct random vibration fatigue analysis of the cantilever beam. Braccesi.C [8]et al uses frequency domain approach of bimodal stress process to estimate the vibration fatigue life of clamped-clamped beam.Wang et al [9,10] proposed a sample method for estimating the random vibration fatigue life of structures and a frequency method for random vibration fatigue analysis of notched specimen.Li et al [11] proposed a nominal stress method for vibration fatigue life analysis of notched specimens and gave the definition and calculation formulas of the stress mean square concentration factor of notched specimens under dynamic load excitation. Lou [12] devised a prediction model for the vibration fatigue life of blades in combination with the stress field intensity method. Luo et al [13,14] combined the Modified Wöhler Curve Method with the Critical Distance theory, and proposed a fatigue life calculation method for notched structures under random load and also formulated a damage gradient model for life prediction.

It is well accepted that the fatigue strength of components depends not only on the maximum stress at the dangerous spots, but also on the stress field distribution in the critical regions. Neuber [15] proposed to take the effective stress as the average value of elastic stress within a certain distance from the notch root. Along the same lines, Peterson [16] took as the effective stress at a certain point within a certain distance from the notch root. Taylor formulated a unified critical distance theory (known as the TCD) based on the above ideas. Susmel et al. have carried out systematic theoretical exploration and experimental verification involving the simplest formalizations of the TCD, i.e. the Line Method (LM) and Point Method (PM). Further, the TCD has been applied successfully to: the life analysis of torsional load fatigue [17], variable loading fatigue [18] and multiaxial loading fatigue [19-21], prediction of static failure [22], determination of critical distance related parameters [23] and influence of mean stress effect [24]. Thanks to its accuracy and reliability, the TCD has become an important theory for fatigue and fracture analysis [25].

In this paper, the TCD is reformulated to make it suitable for calculating the random vibration fatigue life of notched components. In particular, this approach is formalized so that it can be used to assess those situations involving random vibration load spectra with different orders of load magnitude and different bandwidths. In order to assess the accuracy of this alternative formulation of the TCD, a systematic experimental investigation was carried out under random vibration fatigue loading by testing edge notched specimens of 2A12, central circular hole notched specimens of 2A12 and elliptical hole notched specimens of 2024-T3. The obtained results were seen to be promising, confirming that the TCD can be used successfully also to predict vibration fatigue lifetime of notched components.

## 2. TCD METHOD FOR RANDOM VIBRATION FATIGUE LIFE ANALYSIS OF NOTCHED SPECIMENS

According to the TCD, the parameter controlling the fatigue life in the presence of a stress concentrator is the equivalent stress $\sigma_{eff}$ at a distance equal to $D_{PM}$ from the notch root (see Figure 1):

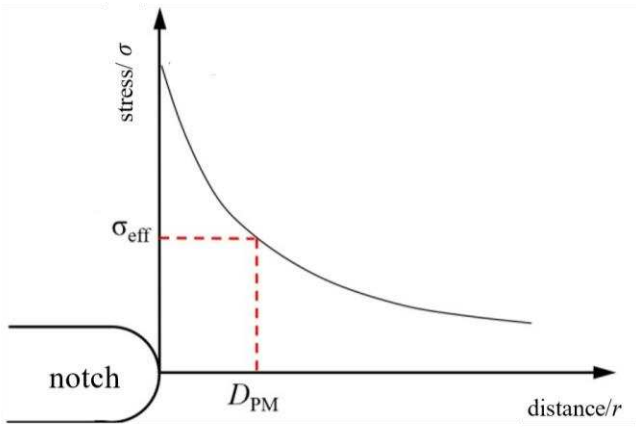


**FIGURE 1** Schematic diagram of critical distance method - point method

$$\sigma_{eff} = \sigma(r = D_{PM}) \tag{1}$$

In Figure 1 and Eq. (1) $\sigma(r)$ is the stress distribution function characterizing the notch under investigation, $r$ is the distance from the notch root, and $D_{PM}$ is the critical distance value calculated as [26,27]:

$$D_{PM} = \frac{1}{2\pi}\left(\frac{\Delta K_{th}}{\Delta\sigma_0}\right)^2 \tag{2}$$

In Eq. (2) $\Delta K_{th}$ is the threshold value of the stress intensity factor of the material and $\Delta\sigma_0$ is the fatigue limit of the material.

According to Miner's linear cumulative damage theory, fatigue damage in notched specimens under variable amplitude load can be estimated as [28]:

$$D=\sum D_i=\sum \frac{n_i}{N_i} \tag{3}$$

where $n_i$ represents the number of load cycles at *i-th* stress level, $S_i$, whreas $N_i$ is the fatigue life of the structure when the stress level is $S_i$ and can be obtained from the corresponding *S-N* curve - $N_i$ can be denoted also as $N(S_i)$. For continuously distributed stress states, the number of load cycles within the stress range ($S_i$ , $S_i$+ Δ $S_i$) is as follows,

$$n_i = vT\sum p(S_i)\Delta S_i \tag{4}$$

where $v$ is the number of stress cycles per unit time, $p(S_i)$ is the probability density function of the stress amplitude. Substituting Eq. (4) into Eq. (3)， it can be obtained

$$\begin{aligned} D &= vT\sum \frac{p(S_i)\Delta S_i}{N_i} \\ &= vT\int_0^\infty \frac{p(S)}{N(S)}\mathrm{d}S \end{aligned} \tag{5}$$

where the probability density function, $p(S)$, of stress amplitude can be calculated by Dirlik model [29].

Here gives the process of Dirlik method:

For random processes, statistical moments $m_i$ can be used to describe the digital characteristics of probability density distribution function (PDF) of random processes, and spectral moments can be used to describe the digital characteristics of power spectral density. The expression of the spectral moment $m_i$ of a stationary process $X$(t) is:

$$m_i = \int_0^\infty \omega^i G(\omega)\mathrm{d}\omega = \int_0^\infty (2\pi f)^i G(f)\mathrm{d}f \tag{6}$$

where $\omega$ is the angular frequency in rad/s and the unit of $f$ is Hz,$G(\omega)$ is the bilateral power spectral density of $X$(t).

The spectral moment $m_i$ can be used to calculate the irregular factor $\gamma$ :

$$\gamma = \frac{m_2}{\sqrt{m_0 m_4}} \tag{7}$$

Dirlik proposed a mixture distribution containing an exponential distribution, two Rayleigh distributions:

$$p(S) = \frac{\frac{D_1}{Q}e^{\frac{-Z}{Q}} + \frac{D_2 Z}{R^2}e^{\frac{-Z^2}{2R^2}} + D_3 Z e^{\frac{-Z^2}{2}}}{\sqrt{m_0}} \tag{8}$$

where

$$D_1 = \frac{2\left(\chi_{\mathrm{m}} - \gamma^2\right)}{1+\gamma^2}, \quad D_2 = \frac{1-\gamma-D_1+D_1^2}{1-R}, \quad D_3 = 1-D_1-D_2$$

$$Z = \frac{S}{\sqrt{m_0}}, \quad Q = \frac{1.25\left(\gamma - D_3 - D_2 R\right)}{D_1}, \quad R = \frac{\gamma-\chi_{\mathrm{m}}-D_1^2}{1-\gamma-D_1+D_1^2}$$

$$\gamma = \frac{m_2}{\sqrt{m_0 m_4}}, \quad \chi_{\mathrm{m}} = \frac{m_1}{m_0}\sqrt{\frac{m_2}{m_4}}$$

Since the aluminum alloy used belongs to the engineering elastic-plastic materials and it is common to use the Mises criterion as the failure criterion, it is appropriate to use Mises stress to express the complex stress state. Under random vibration load, the fatigue damage control parameter of notched specimen is the response Mises stress at the critical distance of $D_{\mathrm{PM}}$. Accordingly, the life $T$ can be obtained from Eq. (5),

$$T = \frac{1}{\nu \int_0^{\infty} \frac{p(\sigma_{\mathrm{PM}})}{N(S)} \mathrm{d}\sigma_{\mathrm{PM}}} \tag{9}$$

where $\sigma_{\mathrm{PM}}$ is the response Mises stress at the critical distance.

## 3. EXPERIMENT

DC-300-3 electric vibration equipment was used for vibration loading. Vibration data processing system RC-2000 was used for the output of spectral response curve of sinusoidal frequency sweep test. The excitation signals of the electric vibration table were detected by the YMC2106C acceleration sensor, which was mounted on the base of the vibration table. The response signal near the mass was treated as the output and gathered by another YMC2106C acceleration sensor. A camera was used to take pictures of the notch root of test specimens every 5 minutes to record and observe the crack initiation process. The testing set-up is shown in Figure 2. In the experiments being run, the time needed to grow (from the notch root) a crack having length equal to 1 mm was taken as the vibration fatigue crack initiation life of the tested specimen.

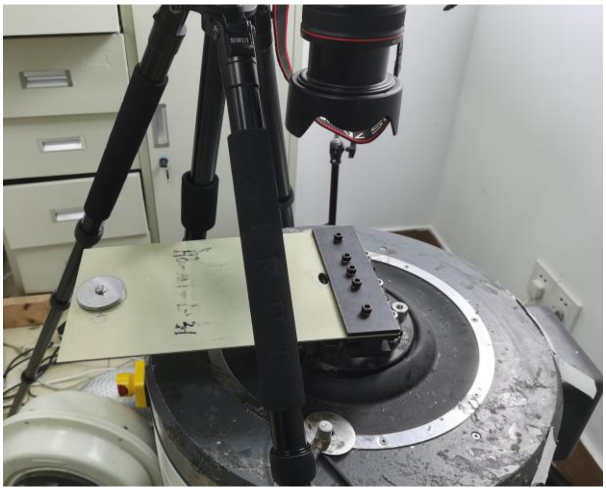

**FIGURE 2** Vibration testing site

### 3.1 Test specimen

The test materials were aluminum alloys 2A12 and 2024-T3. The test specimens were as follows: edge notched specimens of 2A12, center circular hole notched specimens of 2A12 and elliptical hole notched test specimens of 2024-T3. Figure 3 shows the specific dimensions, fixed parts and mass positions of various test specimens being employed.

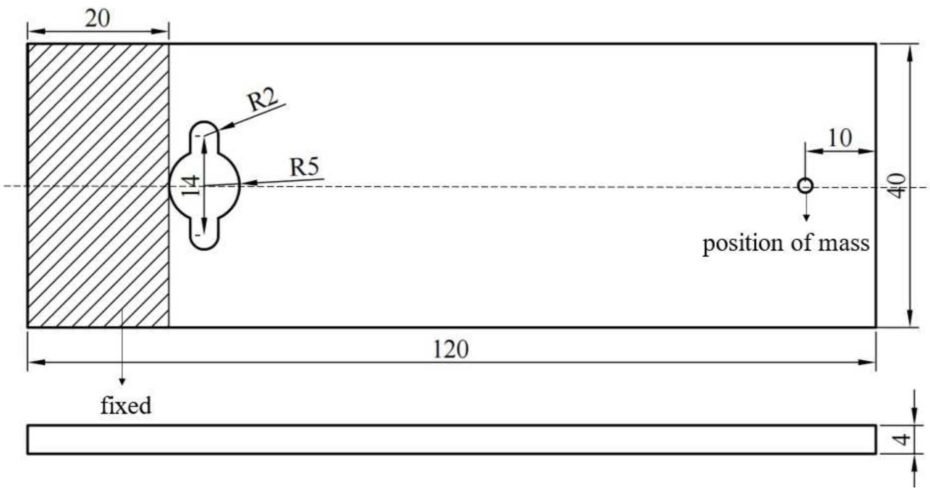


(A)

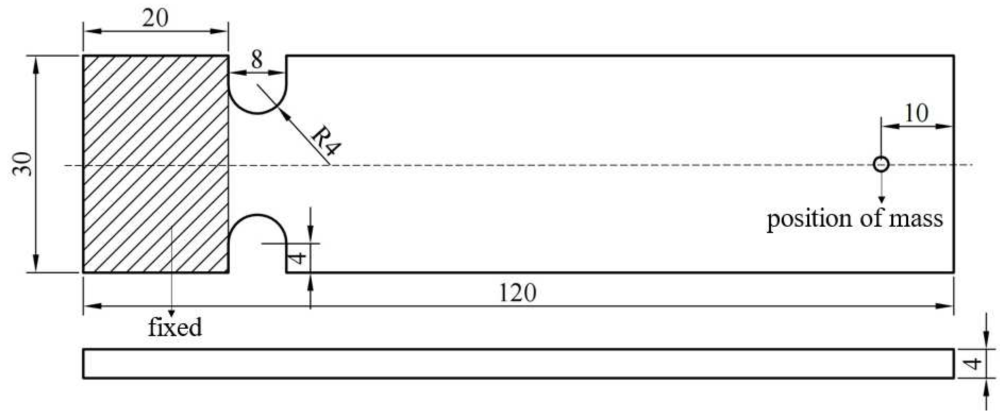


(B)

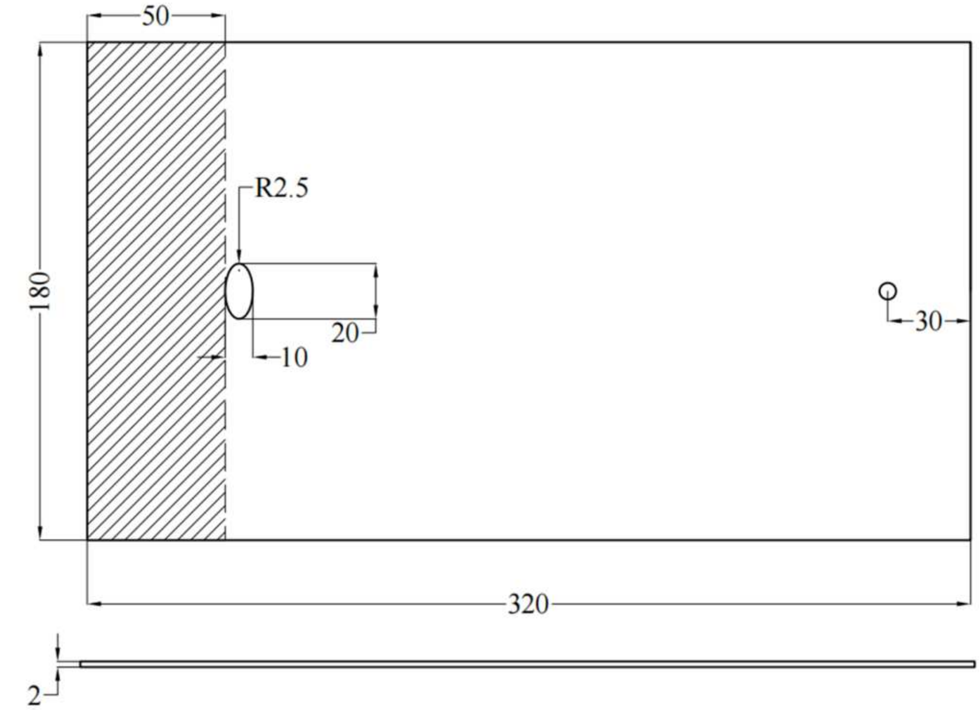


(C)

**FIGURE 3** Test notched specimens(A) Central circular hole notched specimen. (B) Edge notched specimen. (C) Elliptical hole notched specimen

From the geometric dimension diagram of the test piece, it can be known that the notch radii of the above three types of test specimens are 2mm, 4mm and 2.5 mm respectively

### 3.2 Load spectrum test process

During fatigue testing, one end of the test specimen was clamped and the other end was fitted with a mass stack of 200g. Figure 4 shows the installation sketch of a specimen (taking the central circular hole notched test specimen as an example)

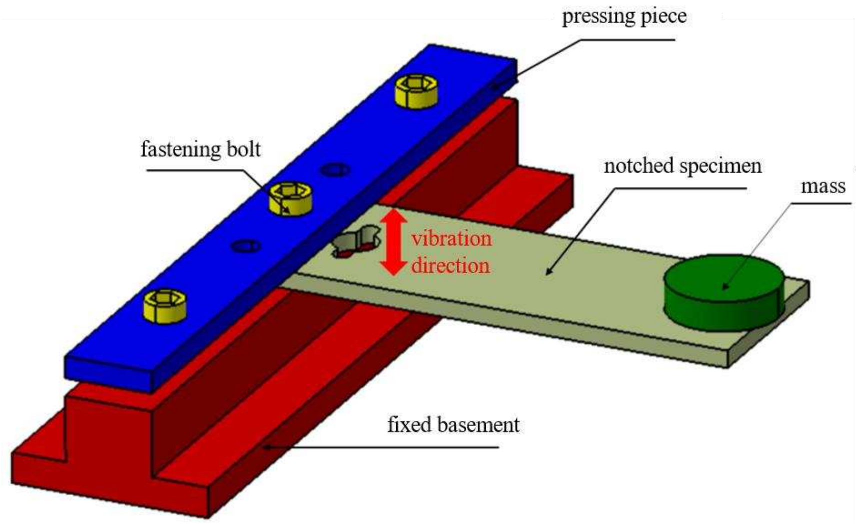


**FIGURE 4** The installation diagram of the central circular hole notched test specimen

Sinusoidal frequency sweep test was carried out for test specimens according to the various testing requirements. The sweep frequency band of central circular hole notched test specimen and edge notched test specimen was in the range 10~1000Hz. In contrast, the sweep frequency band of the elliptical hole notched specimen was in the range 5~200Hz. For all the tests, the sweep frequency acceleration magnitude was 0.1g and the sweep frequency was 1oct/min. The frequency response curve and the first three natural frequencies of the sinusoidal frequency sweep are shown in Figure 5

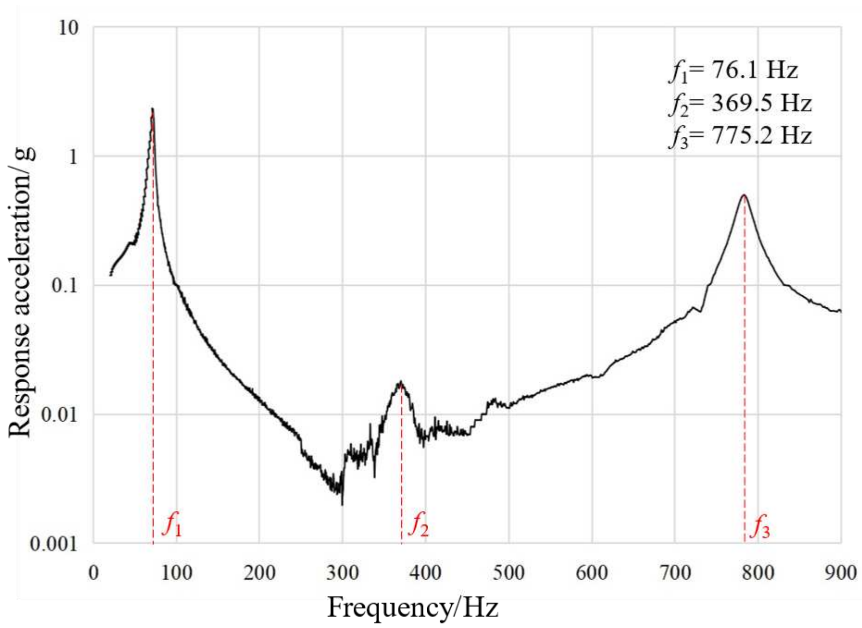


(A)

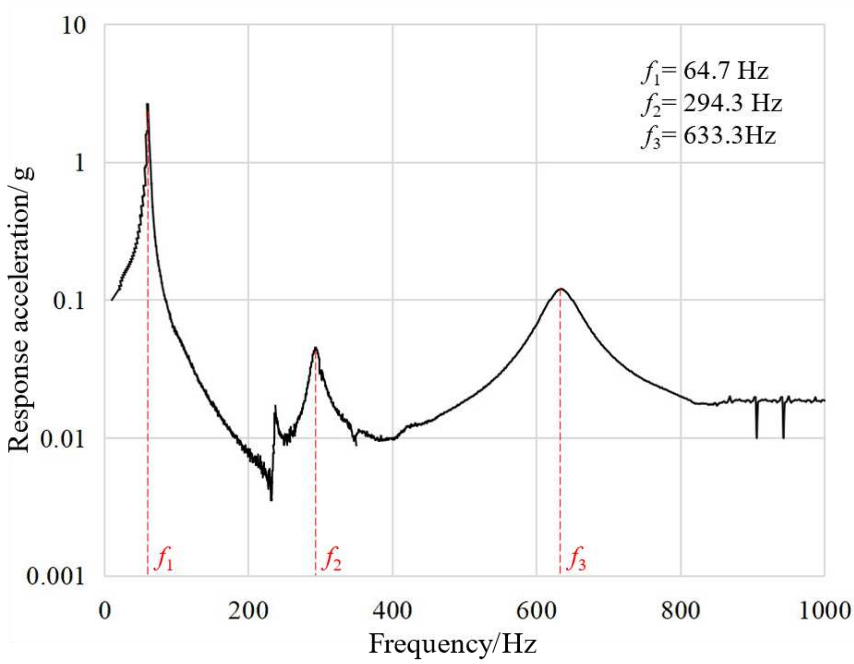


(B)

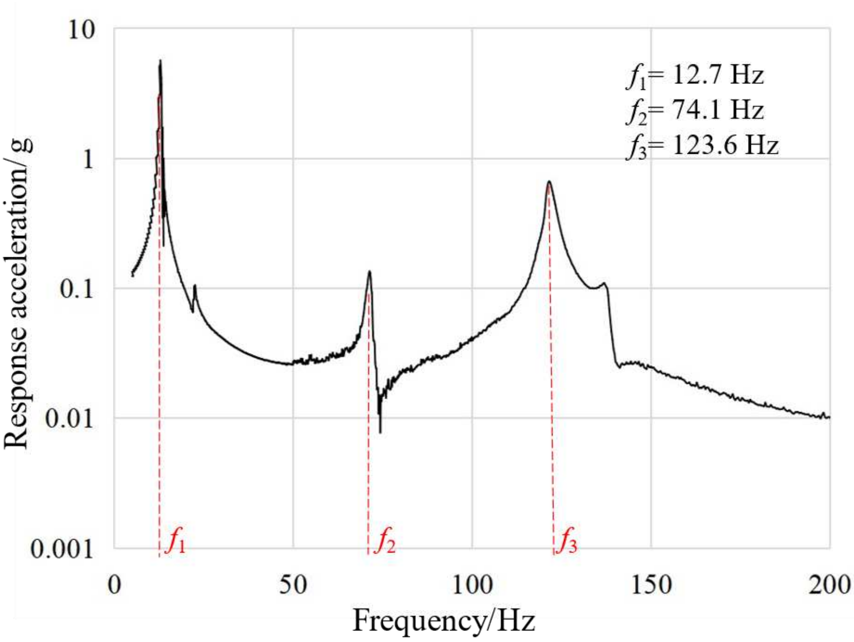


(C)

**FIGURE 5** Sinusoidal frequency sweep response curve and the first three natural frequencies of the central circular hole notched test specimen(A),edge notched test specimen(B) and elliptical hole notched test specimen(C).

According to the natural frequencies obtained from the sinusoidal frequency sweep curves of the notched test specimens, the load excitation spectra were assembled. As shown in Figure 6, the load spectra used for the three geometrical configurations being investigated were straight. This is mainly because this shape of vibration fatigue load spectrum can best reflect the most typical situation of random vibration.

The relevant parameters of the load spectrum are listed in Table 1. The load spectra of the central circular hole notched specimen and the edge notched specimen had the same bandwidth, which contained the first order natural frequency and different acceleration levels. The load spectra of the elliptical hole notched specimens were characterised by the same magnitude, the associated bandwidth being different (covering the first, second, and third order natural frequencies respectively).

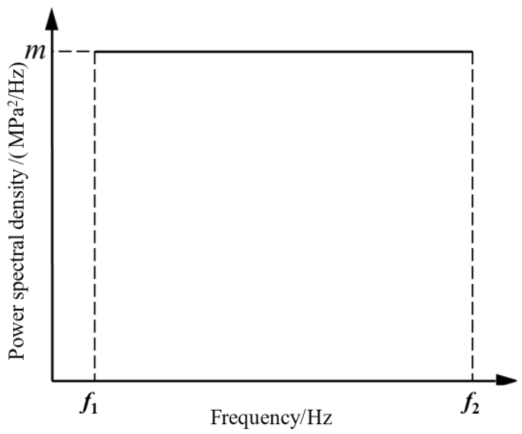


**FIGURE 6** Load spectrum of vibration fatigue test

**TABLE 1** Load spectrum parameters of vibration fatigue test

| Type | Excitation spectrum number | Start frequency $f_1$/Hz | End frequency $f_2$/Hz | Power spectral density magnitude $m$/ (g$^2$/Hz) |
|---|---|---|---|---|
| Edge notched | SS-1 | 10 | 100 | 0.045 |
| | SS-2 | 10 | 100 | 0.050 |
| | SS-3 | 10 | 100 | 0.060 |
| Central circular hole notched | SC-1 | 10 | 100 | 0.080 |
| | SC-2 | 10 | 100 | 0.090 |
| | SC-3 | 10 | 100 | 0.10 |
| Elliptical hole notched | SE-A | 8 | 25 | 0.10 |
| | SE-B | 8 | 90 | 0.10 |
| | SE-C | 8 | 160 | 0.10 |

### 3.3 Test results

The random vibration fatigue tests were conducted as described in the previous section and the test results are listed in Table 2 .

**TABLE 2** Test results of vibration fatigue life

| Type | Excitation spectrum number | Test results of vibration fatigue life /min | | |
|---|---|---|---|---|
| | | Test specimen life $T_{exp}$ | Average $T_{ave}$ | Coefficient of variation/% |
| Edge notched | SS-1 | 81.7、69.1、129.3、84.6 | 91.2 | 25.00 |
| | SS-2 | 72.1、65.4、85.0、71.9 | 73.6 | 9.74 |
| | SS-3 | 60.2、39.9、49.7、42.1 | 48.0 | 16.54 |
| Central circular hole | SC-1 | 115.2、98.4、66.6、70.8 | 87.8 | 22.79 |
| | SC-2 | 44.9、71.2、54.2、75.7 | 61.5 | 20.32 |
| | SC-3 | 32.9、45.5、39.9、60.2 | 44.6 | 22.51 |
| Elliptical hole notched | SE-A | 124.6、124.5、93.7、89.5、85.1、92.6 | 103.5 | 16.83 |
| | SE-B | 91.4、93.5、84.9、89.0、103.4 | 92.4 | 6.69 |
| | SE-C | 73.9、55.2、41.5、90.6、90.4、65.0 | 69.4 | 27.99 |

The failure photos of the three types of notched test specimens are presented in Figure 7.

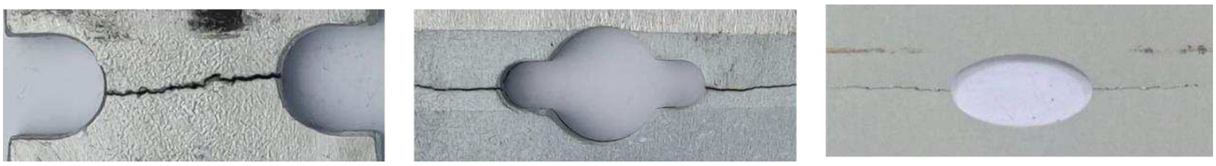

(A) (B) (C)

**Figure 7** Images of broken notched specimens:(A) edge notched specimen. (B) central circular hole notched specimen. (C) elliptical hole notched specimen

From Figure 7, it can be seen that the crack basically propagates from the notch root, and at the initial stage of crack propagation, the crack propagation direction basically follows the angular bisector of the notch root.

## 4. VIBRATION FATIGUE LIFE ANALYSIS

### 4.1 Material properties

This paper assumes that the average stress is 0. The reason is that the stress value of the test specimens used in this paper caused by the gravity of the counterweight is very small compared with the excitation load. For the response stress, although there are non-zero mean stress cycles, through strain collection and time domain simulation in test, we found that the numbers of cycles of positive mean stress basically corresponds to that of negative mean stress, so we gave the assumption.

The mechanical properties(mean stress=0) for aluminum alloys 2A12 and 2024-T3 are listed in Table 3 [30, 31].

**TABLE 3** Mechanical parameters of the two materials

| Material | Density $\rho / (\mathrm{g \cdot cm^{-3}})$ | Threshold value of stress intensity factor $\Delta K_{\mathrm{th}} / (\mathrm{MPa \cdot \sqrt{m}})$ | Material fatigue limit $\Delta\sigma_0$ / MPa | Young's modulus $E$ / GPa |
|---|---|---|---|---|
| 2A12 | 2.78 | 4.74 | 105 | 70 |
| 2024-T3 | 2.73 | 6.98 | 114 | 72 |

The *S-N* curves associated with the two investigated materials are as follows：

$$\begin{array}{ll} \text{2A12 aluminium alloy} & N = 6.95 \times 10^{20} \cdot S^{-7.14} \\ \text{2024-T3 aluminium alloy} & N = 10^{13.8} \cdot (S\text{-}74)^{-4.0} \end{array} \quad (10)$$

According to Eq (2), the material critical distances ($D_{\mathrm{PM}}$) for 2A12 and 2024-T3 aluminum alloys were 0.324 and 0.596 mm, respectively.

### 4.2 Finite Element analysis

By using Patran, 2D finite element modeling was carried out for the three geometrical configurations being investigated(see Fig 9).

The reason for using 2D element is that the thickness of the vibration test specimens used is very small compared with other geometric dimensions of specimens, the test specimen can be considered as a thin plate, and the plane stress assumption is used for FEM. In addition, in the process of vibration test, the crack occurs on the surface of specimens, and then extends to the neutral plane along the thickness direction and the failure criterion is the observation of 1 mm crack initiating in the surface, therefore, the 2D element is appropriate for analysis.

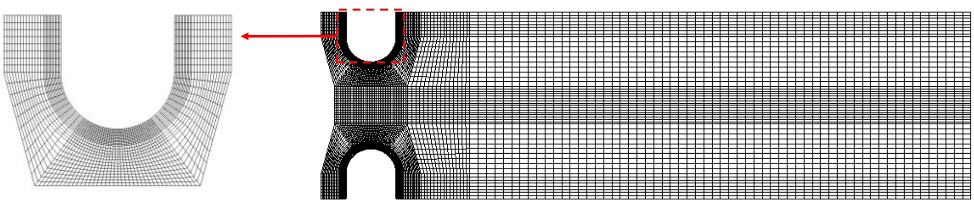

(A)

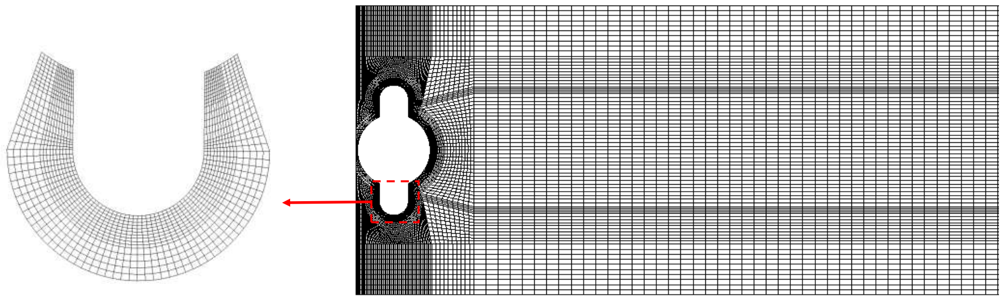

(B)

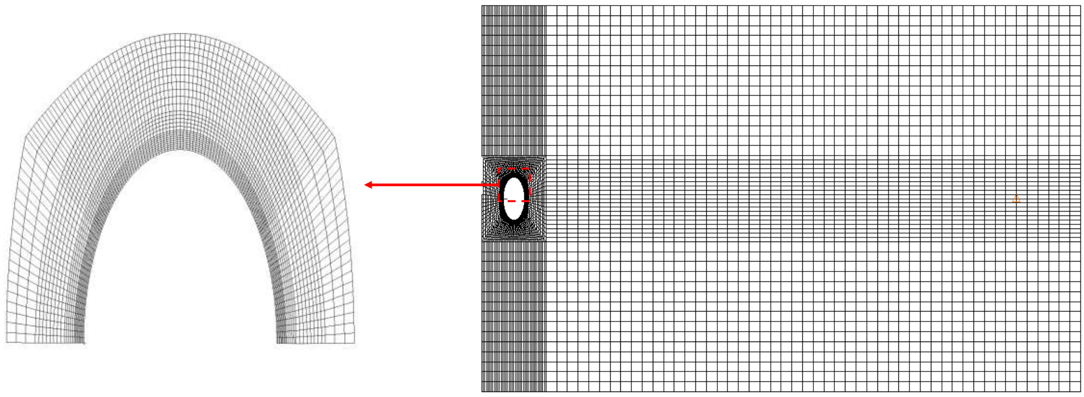

(C)

**FIGURE 8** Local finite element mesh generation of edge notched test specimen (A),central circular hole notched test specimen (B), and elliptical hole notched test specimen (C).

Combined with Nastran, the frequency response analysis can be carried out and the response stress nephogram of the notched specimens at different frequencies can be obtained. Then the RMS distributions of response stress around the notch root under different load spectra can be obtained, which are shown in Figure 9.

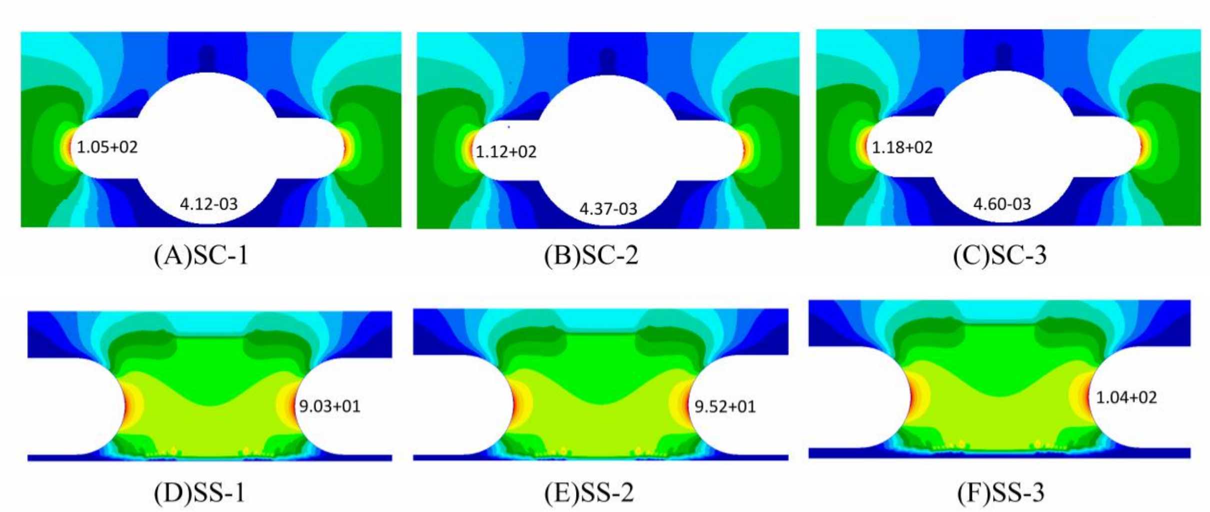

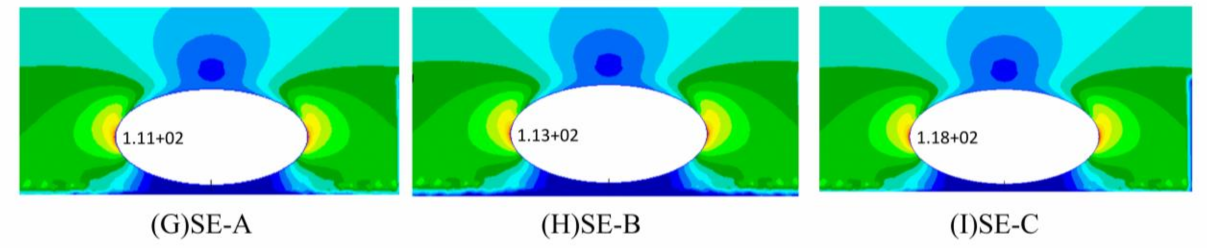


**FIGURE 9** RMS distribution of response stress around the notch root under different load spectra. (A)~(C):central circular hole notched specimen;(D)~(F):edge notched specimen;(G)~(I):elliptical hole notched specimen.

The maximum RMS stress line around the notch root is drawn, which is shown in Figure 10.

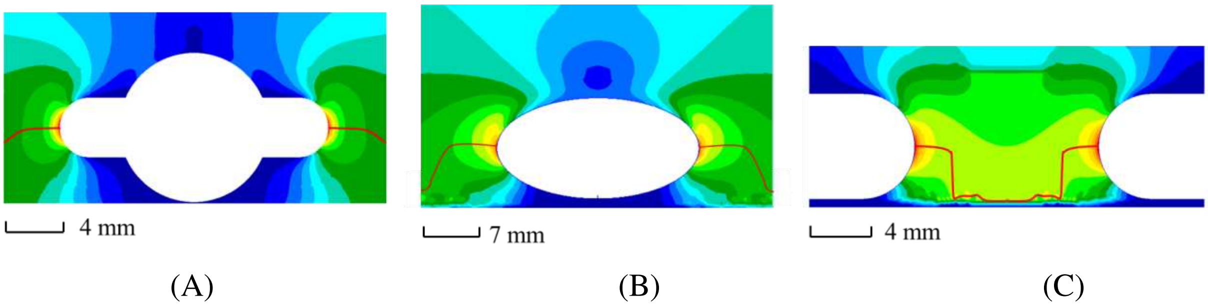


**FIGURE 10** Maximum RMS stress line around the notch root (A)central circular hole notched specimen;(B) elliptical hole notched specimen;(C) edge notched specimen.

From Figure.10 it can be seen that the maximum RMS stress line in the range of critical distance basically coincides with the angular bisector of the notch root. Comparing Figure 10 with Figure 7, it can be concluded that the crack propagation directions of the three kinds of test specimens also follow the angular bisector of the notch root at the initial stage, which is chosen as the critical distance direction.

Therefore, according to TCD theory, the critical-distance point is taken with the value of $D_{PM}$ along the bisector direction of the notch root.

Next, we can obtain the response Mises stress spectra at the critical-distance point under different load spectra by using Patran's random analysis function: stress spectra are shown in Figure 11 and some detailed parameters of the spectra are included in Table 4.

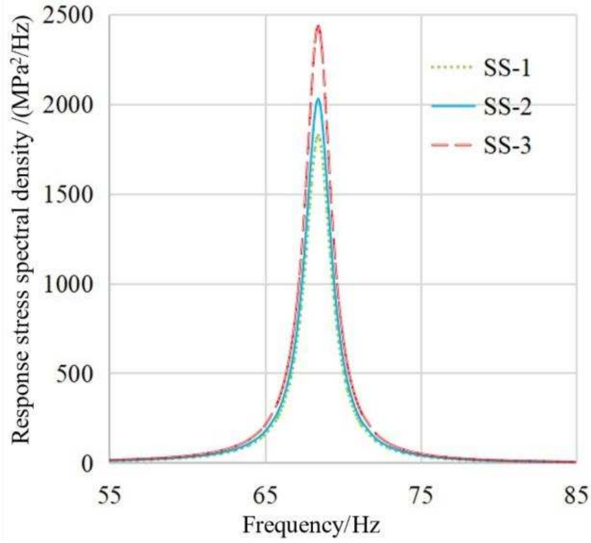

Response stress spectral density /(MPa²/Hz)
2500
2000
1500
1000
500
0
55
65
75
85
Frequency/Hz
SS-1
SS-2
SS-3


(A)

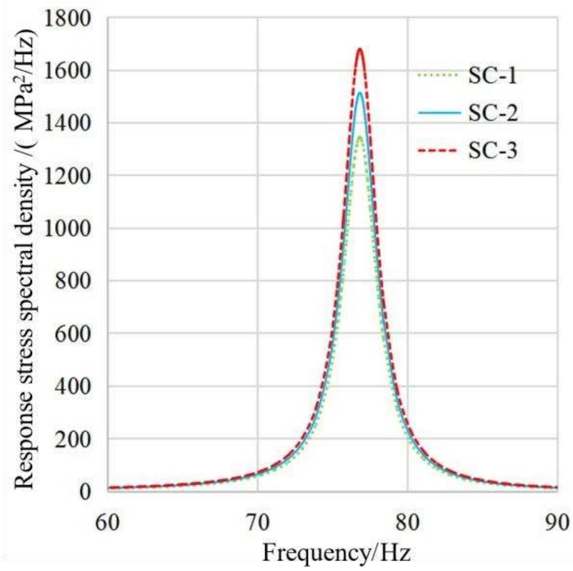

Response stress spectral density /( MPa²/Hz)
1800
1600
1400
1200
1000
800
600
400
200
0
60
70
80
90
Frequency/Hz
SC-1
SC-2
SC-3


(B)

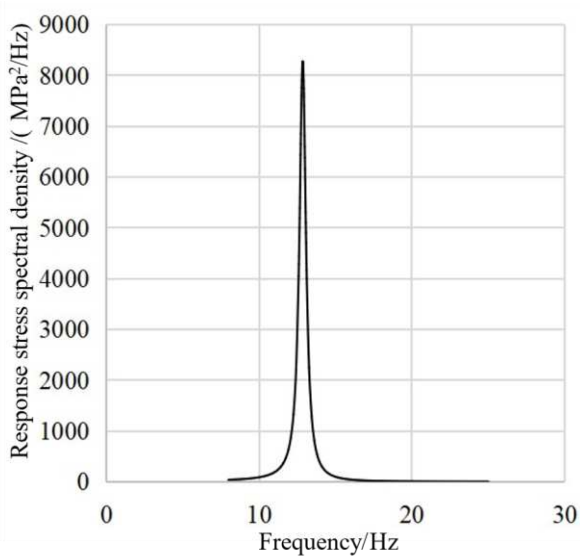

Response stress spectral density /( MPa²/Hz)
9000
8000
7000
6000
5000
4000
3000
2000
1000
0
0
10
20
30
Frequency/Hz


(C)

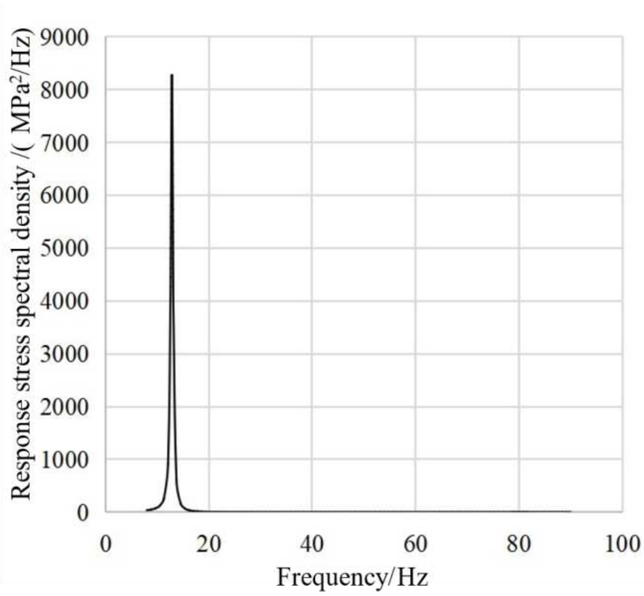

Response stress spectral density /( MPa²/Hz)
9000
8000
7000
6000
5000
4000
3000
2000
1000
0
0
20
40
60
80
100
Frequency/Hz


(D)

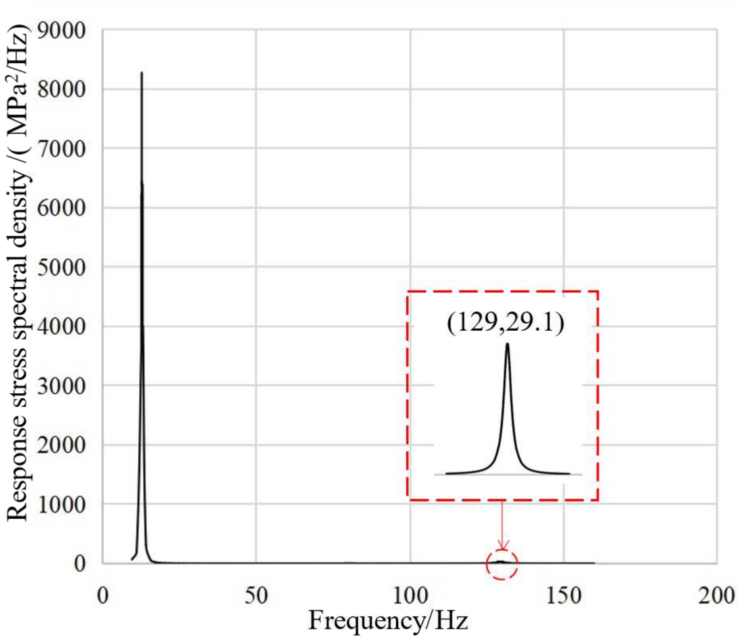


(E)

**FIGURE 11** (A) Response Mises stress spectra of edge notched test specimen at critical distance under different load spectra. (B) Response Mises stress spectra of central circular hole notched test specimen at critical distance under different load spectra. (C) Response Mises stress spectra of elliptical hole notched test specimen at critical distance under SE-1 load spectrum. (D) Response Mises stress spectra of elliptical hole notched test specimen at critical distance under SE-2 load spectrum.(E) Response Mises stress spectra of elliptical hole notched test specimen at critical distance under SE-3 load spectrum

**TABLE 4** Response stress spectra under different excitation spectra

| Type | Excitation spectrum number | Peak of stress PSD ($MPa^2.Hz^{-1}$) | RMS value of stress/MPa |
|---|---|---|---|
| Edge notched | SS-1 | 1.83e+3 | 76.5 |
| | SS-2 | 2.03e+3 | 80.6 |
| | SS-3 | 2.44e+3 | 88.3 |
| Central circular hole notched | SC-1 | 1.34e+3 | 76.3 |
| | SC-2 | 1.51e+3 | 80.9 |
| | SC-3 | 1.68e+3 | 85.2 |
| Elliptical hole notched | SE-A | 8.28e+3 | 90.3 |
| | SE-B | 8.28e+3 | 92.1 |
| | SE-C | 8.28e+3 | 96.9 |

It can be seen from Table 4 that with the increase of the magnitude of the power spectrum density of the excitation load spectrum, the root mean square value RMS and the peak value of the response stress spectrum increase. With the increase of the band width of the excitation load spectrum, the root mean square value RMS of the response stress spectrum increases and the peak value basically remains unchanged.

As seen in Figure 12, the probability distribution of the stress amplitude was determined by substituting the response Mises stress spectra of the three notch configurations under the investigated load spectra into the Dirlik model.The whole process is carried out in Matlab.

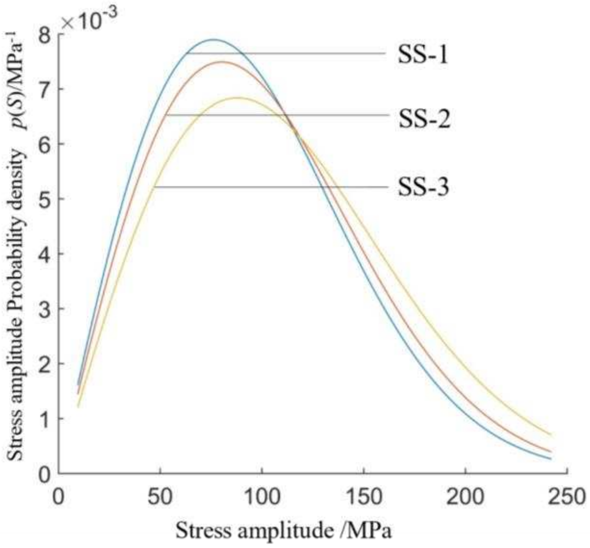


(A)

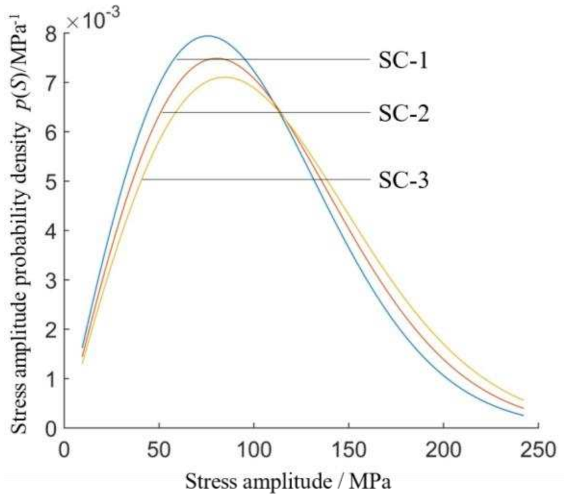


(B)

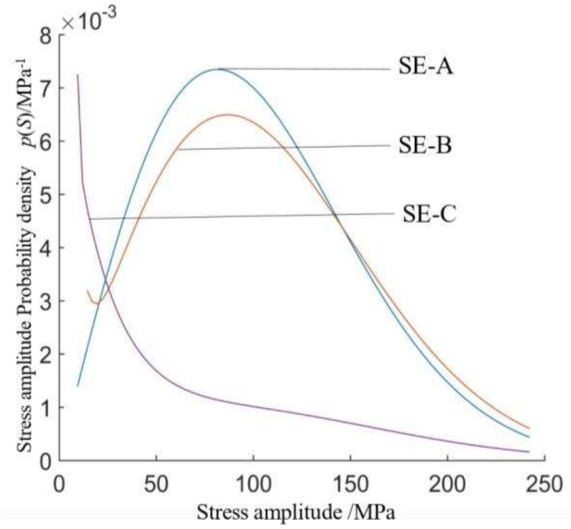


(C)

**FIGURE 12** Probability density function of stress amplitude of notched test specimen under different load spectra:(A) edge notched test specimen. (B) central circular hole notched test specimen. (C) elliptical hole notched test specimen

### 4.3 TCD method of life prediction

Combined with the finite element simulation model, the response Mises stress spectrum at the critical distance was obtained. Then the Dirlik model was used to fit the probability distribution of the stress amplitude, $p(S)$. Subsequently, the $p(S)$ and the *S*-*N* curve denoted in Eq. (8) (10) were substituted into the Eq. (9) to calculate the random vibration fatigue life. The calculation results are shown in Table 5 below. The error factor, $\eta$, listed in the Table 4 was calculated as follows:

$$\text{Error factor } \eta = \frac{\text{Experimental life } T_{\text{exp}}}{\text{Calculated life } T_{\text{cal}}} \tag{11}$$

It can be seen from the formula that the error factor reflects the error magnitude and the conservative degree of prediction. It should be noted that when the error factor is >1, the calculated life is conservative. In contrast, when the error factor is<1, the calculated life is non-conservative.

**TABLE 5** Test results of vibration fatigue life and prediction error

| Type | Excitation | Vibration fatigue life/min | Error factor |
|---|---|---|---|

| | spectrum number | Experiment $T_{exp}$ | Calculation $T_{cal}$ | $\eta$ |
|---|---|---|---|---|
| Edge notched | SS-1 | 91.2 | 92.8 | 0.98 |
| | SS-2 | 73.6 | 64.5 | 1.14 |
| | SS-3 | 48.0 | 34.5 | 1.39 |
| Central circular | SC-1 | 87.8 | 85.3 | 1.03 |
| | SC-2 | 61.5 | 56.9 | 1.08 |
| | SC-3 | 44.6 | 39.8 | 1.12 |
| Elliptical hole | SE-A | 101.6 | 81.4 | 1.25 |
| | SE-B | 92.4 | 60.5 | 1.53 |
| | SE-C | 69.4 | 31.3 | 2.20 |

It can be seen from Table 5 that the error factor increases with the increase of the acceleration excitation level and the broadening of the frequency band of load spectra. This is mainly because, with the increase of the loading level, the proportion of large load in the load cycles increases, and the widening of the frequency band causes superposition of multiple modal vibration shapes of notched specimens, which will exacerbate the nonlinearity of vibration while the finite element analysis is based on the linear hypothesis. Hence, the error factor shows a gradual increase trend.

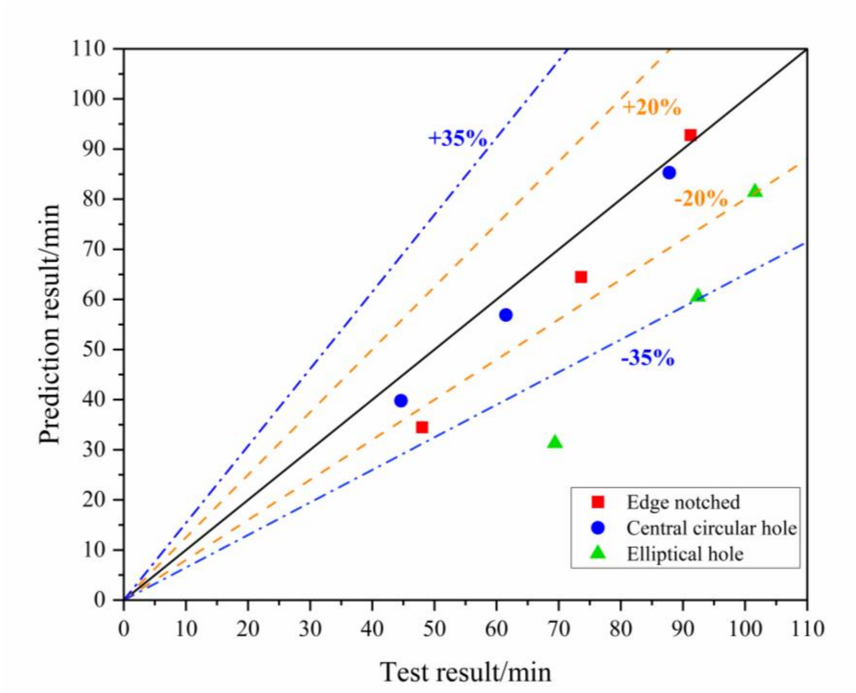


**FIGURE 13** Comparative analysis of test value and predicted value

It can be seen from Figure 13 that almost all the data show conservative predictions and most of the predicted values fall within the 20% error band. Therefore, the TCD has been validated as an effective method for predicting the random vibration fatigue life of notched specimens.

## 5. DISCUSSION

(1) Compared to the other two test pieces, the estimated vibration fatigue life of the elliptical hole test specimen is more conservative. This is because the load spectra (SE-B, SE-C) of the elliptical hole specimens span the first two or three natural frequencies of the test specimens and the load spectral bandwidth are larger than that of the other two kinds of specimens.

The widening of the load spectrum bandwidth increases the number of load cycles per unit time. Due to the thin plate structure of the test specimens, there is a certain degree of decrease in stiffness following under high frequency vibration, which will make the number of response stress cycles per unit time slightly less than that of excitation load cycles. In this case, the fatigue damage of the test is overestimated, which makes the calculation value more conservative. This is also the reason why the life of the load spectrum SE-C shows relatively large error.

(2) Most fatigue lives estimated by the paper's method based on TCD are conservative, which is practical to engineering because the estimated non-conservative value is dangerous. It also proves the effectiveness of the method in this paper.

(3) It needs to be noted that although theoretically speaking, the radius of notch or defect has some influence on fatigue life analysis, the TCD model used for vibration fatigue analysis has little or no relationship with the radius or defect of notch. This is mainly because the TCD model used in this paper initially uses the equivalent stress at the critical distance from the notch root to characterize the damage of material and the critical distance has little relationship with the radius or defect of notch, therefore the method is independent of the radius or defect of notch, which is also one of the advantages.

## 6. CONCLUSIONS

(1) In this paper, the TCD method for random vibration fatigue life analysis of notched specimens is proposed. The response Mises stress spectrum at the critical distance is used as the characterization parameter of stress distribution and stress magnitude near the notch root under random vibration excitation. The idea is clear and the calculation efficiency is high.

(2) The method proposed in this paper takes into account the random vibration load spectrum of different orders of magnitude and different bandwidths, and has a wide range of applicability. Comparing the life prediction results with the test results, the prediction accuracy is high.

(3) The method introduces structural dynamic characteristics by using response stress spectra and considers the stress distribution around the notch root by applying TCD. It is proved that the application of TCD to vibration fatigue is reasonable.

## ACKNOWLEDGEMENT

The National Natural Science Foundation of China (Grant No. 52075244) is acknowledged for supporting the present research.

## CONFLICT OF INTEREST

The authors declare that they have no known competing financial interests or personal relationships that could have appeared to influence the work reported in this paper.

## REFERENCES

[1] Yao WX. *Fatigue Life Estimation of Structures*. Science Press; 2019. (in Chinese)

[2] Yao WX, Ye B, Zheng L-C. A verification of the assumption of anti-fatigue design. *Int. J. Fatigue* 2001; 23(1):271-277.

[3] Yao WX, Xia KQ, Gu Y. On the fatigue notch factor $K_f$. *Int. J. Fatigue* 1995; 17(4):245-251.

[4] Yao WX. The description for fatigue behaviours of metals by stress field intensity approach. *Acta mech. solida sin*. 1997;8(1):38-48. (in Chinese)

[5] Taylor D. Geometrical effects in fatigue：A unifying theoretical model. *Int. J. Fatigue* 1999;21：413-420.

[6] Taylor D. The Theory of Critical Distances: a new perspective in fracture mechanics. Elsevier 2007.

[7] Wirsching PH, Light MC. Fatigue under wide band random loading. J Struct Div, ASCE 1980;106(7):1593-1607

[8] Braccesi C, Cianetti F, Lori G, et al. Fatigue behaviour analysis of mechanichal components subject to random bimodal stress process:frequency domain approach. *Int. J. Fatigue* 2005;27:335-345.

[9] Wang MZ, Yao WX, Sun W. Sample approach for fatigue life prediction of structures under random vibration. Chinese Journal of Construction Machinery.2008;19(8):972:975.

[10] Wang MZ, Yao WX. Frequency domain method for fatigue life analysis on notched specimens under random vibration loading

[11] Li DY, Yao WX. Nominal stress approach for life prediction of notched specimen under vibration loading. *Acta Aeronautica et Astronautica Sinica* 2011;32(11):2036-2041. (in Chinese)

[12] Lou GK. Research on probability life prediction of blade vibration fatigue. Nanjing University of Aeronautics and Astronautics, 2020. (in Chinese)

[13] Luo ZB, Chen HH, Wang J, et al. Fatigue life calculation of notched specimens by modified Wöhler curve method and theory of critical distance under multiaxial random loading. *Fatigue Fract. Eng. Mater. Struct.* 2020;43(9):2101-2115.

[14] Luo ZB, Chen HH, Zheng RH , et al. A damage gradient model for life prediction of notched metallic structures under multiaxial random vibrations. *Fatigue Fract. Eng. Mater. Struct.*2021;45(2):514-529.

[15] Neuber H. Theory of notch stresses: principles for exact calculation of strength with reference to structural form and material. *2nd ed. Berlin: Springer*, 1958.

[16] Peterson RE. Notch sensitivity. Metal fatigue, 1959:293-306

[17] Susmel L, Taylor D. A simplified approach to apply the theory of critical distances to notched components under torsional fatigue loading. *Int. J. Fatigue* 2006;28:417-430.

[18] Susmel L, Taylor D. The Theory of Critical Distances to estimate lifetime of notched components subjected to variable amplitude uniaxial fatigue loading. *Int. J. Fatigue* 2011;33(7):900-911.

[19] Susmel L, Taylor D. Non-propagating cracks and high-cycle fatigue failures in sharply notched specimens under in-phase Mode I and II loading. *Eng. Fail. Anal.* 2007;14: 861–876.

[20] Susmel L. Modified Wöhler curve method, theory of critical distances and Eurocode 3: A novel engineering procedure to predict the lifetime of steel welded joints subjected to both uniaxial and multiaxial fatigue loading. *Int. J. Fatigue* 2008;30: 888–907.

[21] Susmel L. The Modified Wöhler Curve Method calibrated by using standard fatigue curves and applied in conjunction with the Theory of Critical Distances to estimate fatigue lifetime of aluminium weldments. *Int. J. Fatigue* 2009;31:197–212.

[22] Susmel L, Taylor D. On the use of the Theory of Critical Distances to predict static failures in ductile metallic materials containing different geometrical features. *Eng. Fract. Mech.* 2008;75:4410–4421.

[23] Susmel L, Taylor D. The Theory of Critical Distances as an alternative experimental strategy for the determination of $\Delta K_{IC}$ and $\Delta K_{th}$. *Eng. Fract. Mech.* 2010;77:1492–1501.

[24] Susmel L, Atzori B, Meneghetti G, Taylor D. Notch and mean stress effect in fatigue as phenomena of elasto-plastic inherent multiaxiality. *Eng. Fract. Mech.* 2011;78:1628–1643.

[25] Susmel L. The theory of critical distances: a review of its applications in fatigue. *Eng. Fract. Mech.* 2008;75:1706-1724.

[26] Frost NE. Significance of Non-propagating Cracks in the Interpretation of Notched Fatigue Data. *J. Mech. Eng. Science* 1961;3(4):299-302.

[27] El Haddad MH, Smith KN, Topper TH. Fatigue crack propagation of short cracks. ASME. *J. Eng. Mater. Technol.* 1979;101(1):42-46.

[28] Tovo R. Cycle distribution and fatigue damage under broad-band random loading. *Int. J. Fatigue* 2002;24:1137-1147.

[29] Dirlik T. Application of computers in fatigue analysis. Engineering University of Warwick Coventry, England.1985,1.

[30] Ding CF, Yu H, Wu XR. Investigation of threshold and wide range fatigue crack propagation rates in LY12CZ alloy. *J. Aeronautical Mater*. 2000;20(1):12-17. (in Chinese)

[31] Liu JZ, Lou RX. *Data sheet on mechanical properties of key Metal Materials for aircraft design.Beijing*. Aviation Industry Press.2015. (in Chinese)